J. Biochem. 2012;152(2):149–159 doi:10.1093/jb/mvs054

JB THE JOURNAL OF BIOCHEMISTRY

Physical and functional interaction of the active zone protein CAST/ERC2 and the β-subunit of the voltage-dependent Ca^{2+} channel

Received January 30, 2012; accepted March 24, 2012; published online May 9, 2012

Shigeki Kiyonaka[1,2,3], Hiroshi Nakajima[1], Yoshinori Takada[1], Yamato Hida[4], Toshinori Yoshioka[4], Akari Hagiwara[4], Isao Kitajima[5], Yasuo Mori[1,2,3] and Toshihisa Ohtsuka[4,*]

[1]Laboratory of Molecular Biology, Department of Synthetic Chemistry and Biological Chemistry, Graduate School of Engineering; [2]Laboratory of Environmental Systems Biology, Department of Technology and Ecology, Hall of Global Environmental Studies, Kyoto University, Kyoto 615-8510; [3]CREST, JST, Tokyo 102-0075; [4]Department of Biochemistry, Graduate School of Medicine/Faculty of Medicine, University of Yamanashi, Yamanashi 409-3898; and [5]Department of Clinical and Molecular Pathology, Faculty of Medicine/Graduate School of Medicine, University of Toyama, Toyama 930-0194, Japan

*Toshihisa Ohtsuka, Department of Biochemistry, Graduate School of Medicine/Faculty of Medicine, University of Yamanashi, 1110 Shimokato, Chuo, Yamanashi 409-3898, Japan, Tel: +81 55 273 6740, Fax: +81 55 273 6740, email: tohtsuka@yamanashi.ac.jp

In the nerve terminals, the active zone protein CAST/ERC2 forms a protein complex with the other active zone proteins ELKS, Bassoon, Piccolo, RIM1 and Munc13-1, and is thought to play an organizational and functional role in neurotransmitter release. However, it remains obscure how CAST/ERC2 regulates the Ca^{2+}-dependent release of neurotransmitters. Here, we show an interaction of CAST with voltage-dependent Ca^{2+} channels (VDCCs), which are essential for regulating neurotransmitter release triggered by depolarization-induced Ca^{2+} influx at the active zone. Using a biochemical assay, we showed that CAST was coimmunoprecipitated with the VDCC β_4-subunit from the mouse brain. A pull-down assay revealed that the VDCC β_4-subunit interacted directly with at least the N- and C-terminal regions of CAST. The II–III linker of VDCC α_1-subunit also interacted with C-terminal regions of CAST; however, the interaction was much weaker than that of β_4-subunit. Furthermore, coexpression of CAST and VDCCs in baby hamster kidney cells caused a shift in the voltage dependence of activation towards the hyperpolarizing direction. Taken together, these results suggest that CAST forms a protein complex with VDCCs, which may regulate neurotransmitter release partly through modifying the opening of VDCCs at the presynaptic active zones.

Keywords: CAST/CAZ protein/presynaptic active zone/β-subunit/voltage-dependent Ca^{2+} channel.

Abbreviations: aa, amino acid; Ab, antibody; BHK, baby hamster kidney; Brp, Bruchpilot; CBB, Coomassie brilliant blue; CSM, crude synaptic membrane; GST, glutathione *S*-transferase; HEK, human embryonic kidney; IP, immunoprecipitation; VDCC, voltage-dependent Ca^{2+} channel; WB, Western blotting.

The presynaptic active zone is a specialized site for neurotransmitter release in the nerve terminals, which is characterized by its high-electron density under electron microscopy (*1*). Recent biochemical and molecular biological approaches have identified active zone-specific proteins including CAST/ERC2 (*2*, *3*), ELKS (*3*, *4*), Bassoon (*5*), Piccolo/Aczonin (*6*, *7*), Munc13-1 (*8*) and RIMs (*9*). Among them, CAST and ELKS consist of a small family containing several coiled-coil domains and a unique C-terminal three-amino acid motif [Ile–Trp–Ala (IWA)] (*2*, *3*). CAST forms a large molecular complex through direct binding to ELKS, Bassoon, Piccolo and RIM1, and indirect binding to Munc13-1 (*10*), which might be the molecular basis for the electron density of the active zone cytomatrix (*11*).

Disruption of the CAST and Bassoon or RIM1 interaction significantly impairs synaptic transmission in cultured ganglion neurons (*10*). In *Drosophila*, knockdown of Bruchpilot (Brp), a homologue of the ELKS/CAST family, results in the disappearance of the active zone cytomatrix, also called T-bar, and significantly perturbs evoked neurotransmission (*12*, *13*). The family member ELKS has also been reported to regulate exocytosis. For instances, overexpression of ELKS causes a significant increase in stimulated exocytosis of human growth hormone in PC12 cells (*14*), which is mediated at least in part via the RIM1-Munc13-1 pathway. In addition, using total internal reflection fluorescence microscopy, it has been shown that disruption of the ELKS and Bassoon binding reduces the docking and fusion of insulin granules, and attenuation of ELKS expression by small interfering RNA reduces the glucose-evoked insulin release, suggesting its role in insulin exocytosis from pancreatic β cells (*15*). More recently, it has been demonstrated with CAST/ERC2 knockout mice that CAST/ERC2 deletion does not change the number of docked vesicles or other ultrastructural synapse parameters, but it causes a large increase in inhibitory, but not excitatory, neurotransmitter release (*16*). Despite the different systems employed, these accumulated observations suggest that CAST plays a pivotal

role in neurotransmitter release from the active zone; however, its functional linkage with voltage-dependent Ca^{2+} channels (VDCCs) still remains obscure.

In the mammalian neural system, VDCCs such as the N-, P/Q-, R- and L-type play essential roles in neurotransmitter release from presynaptic nerve terminals (*17–19*). VDCCs are characterized as heteromultimeric protein complexes composed of the pore-forming α_1-subunit and the auxiliary α_2/δ-, β- and γ-subunits (*20*). These VDCC complexes are known to associate with presynaptic and postsynaptic proteins including syntaxin, SNAP-25, synaptotagmin, CASK and Mint through interactions with the α_1-subunit (*21–30*). Among the auxiliary subunits, the β-subunits interact with the α_1-subunit in the cytoplasm to enhance functional channel trafficking to the plasma membrane (*31*, *32*) and to modify multiple kinetic properties (*33*, *34*). There are four subfamilies of β-subunits (β_1–β_4), each with splice variants, encoded by four distinct genes. Recently, several β-subunit-binding proteins have been identified and characterized (*35–41*). For example, the active zone protein RIM1 has been shown to interact directly with the β-subunit and sustain Ca^{2+} influx through inhibition of channel inactivation (*40*, *41*). RIM1 also associates with the α_1-subunit and anchors VDCCs to the active zones (*42*, *43*). In *Drosophila*, Brp is essential for clustering VDCCs (*12*). Thus, we are beginning to understand the molecular relationship between the VDCC complexes and the active zone proteins.

In this study, to obtain further insight into the linkage between active zone proteins and VDCC functions, we have analysed the physical and functional interactions between CAST and VDCCs. Biochemical studies showed that CAST interacts directly with the β-subunit of VDCC *in vitro* and *in vivo*. Moreover, coexpression of CAST with VDCCs in baby hamster kidney (BHK) cells caused a shift in the voltage dependence of activation towards the hyperpolarizing direction. Taken together, CAST regulates neurotransmitter release partly through modifying the opening of VDCCs at the presynaptic active zones.

Experimental Procedures

cDNAs and vector construction

Expression vectors were constructed in pGEX (Amersham Biosciences, Lettle Chalfont, UK), pET23 (Novagen, Madison, WI, USA), pCMV-HA (*44*), pCI-neo (Promega, Madison, WI, USA), pCMV-tag3 (Stratagene, La Jolla, CA, USA) and pEGFP-C1 (Clontech, Palo Alto, CA, USA) using standard molecular biological methods. Rat β_{4b} (GenBank^{TM} accession number XM_215742) and the BI-2 variant of the rabbit $Ca_v2.1$ (GenBank^{TM} accession number X57477) were used for expression experiments. Other constructs for CAST, RIM1 and C-terminal region of Bassoon (BassoonC) were prepared as previously described (*2*, *10*). RIM1 cDNA was supplied by S. Seino (Kobe University, Japan). Glutathione *S*-transferase (GST) fusion proteins were purified according to the manufacturer's protocol (GE Healthcare, Buckinghamshire, UK).

Antibodies

The antibodies used in this study were mouse monoclonal anti-Myc (9E10; Roche, Mannheim, Germany), anti-HA (12C5A; Roche) and anti-synaptophysin (SY38; Chemicon, Temecula, CA, USA) and rabbit polyclonal anti-GFP (A11122; Invitrogen, Carlsbad, CA, USA), anti-β_4 (*40*), anti-CAST (*2*) and anti-$Ca_v2.1$ (Alomone Labs, Jerusalem, Israel).

Coimmunoprecipitation and pull-down assay using mouse brain lysate

To obtain the crude synaptic membrane (CSM) fraction, subcellular fractionation was performed as previously described (*29*). Whole mouse brains (8 g) were homogenized in a homogenization buffer containing 4 mM HEPES (pH 7.4), 0.32 M sucrose, 5 mM EDTA, 5 mM EGTA and protease inhibitors. Cell debris and nuclei were removed by centrifugation at 800 *g* for 10 min. The supernatant was centrifuged at 9,000*g* for 15 min to obtain the crude synaptosomal fraction in the pellet. Crude synaptosomes were resuspended in the homogenization buffer and centrifuged at 10,000*g* for 15 min. The washed crude synaptosomes were lysed by hypo-osmotic shock in water, rapidly adjusted to 1 mM HEPES/NaOH (pH 7.4), and stirred on ice for 30 min. After centrifugation of the lysate at 25,000*g* for 20 min, the pellet was resuspended in 0.25 M buffered sucrose. The synaptic membranes were then further enriched through a discontinuous sucrose gradient containing 0.8/1.0/1.2 M sucrose. After centrifugation at 65,000*g* for 2 h, the CSM fraction was collected from the 1.0/1.2 M sucrose interface. Synaptic membrane proteins were extracted from the CSM with a solubilization buffer containing 50 mM Tris–Cl (pH 7.4), 500 mM NaCl, a mixture of protease inhibitors and 1% digitonin (Biosynth, Itasca, IL, USA). After centrifugation at 147,600*g* for 37 min, the supernatant was diluted with a buffer containing 50 mM Tris and 0.1% digitonin to adjust the NaCl concentration to 150 mM and incubated overnight at 4°C. Following centrifugation at 17,400*g* for 15 min, the solution including neuronal VDCC complexes was obtained. For coimmunoprecipitation, the solution was incubated with ProteinA Agarose coupled to anti-β_4 antibodies (*40*) at 4°C for 6 h. For the GST pull-down assay, the solution was incubated with glutathione-Sepharose beads containing the indicated GST fusion proteins at 4°C for 1 h. After the beads were extensively washed with buffer, the bound proteins were eluted by boiling the beads in SDS sample buffer for 5 min, or by incubating the beads in SDS sample buffer containing 50 mM DTT for 30 min at room temperature. Samples were then analysed by western blotting.

Pull-down assay using HEK293 cells

HEK293 cells transfected with cDNA plasmids expressing Myc-VDCC β_{4b}, HA-RIM1 or EGFP-BassoonC by Lipofectamin 2000 (Invitrogen) in 10 cm dishes were lysed with 1 ml of buffer containing, 20 mM Tris–Cl (pH 7.5), 150 mM NaCl, 0.5 mM EDTA, 1 mM DTT, 1% (w/v) Triton X-100, 10 μg/ml leupeptin and 10 μM APMSF at 4°C for 1 h. Samples were centrifuged at 20,000*g* at 4°C for 20 min to collect the supernatant. The HA-RIM1 and EGFP-BassoonC samples were diluted 4-fold with the buffer. These 0.5 ml supernatants were then incubated with 20 μl of glutathione-Sepharose beads containing the indicated GST fusion proteins at 4°C for 1 h. After the beads were extensively washed with buffer, the bound proteins were eluted by boiling the beads in SDS sample buffer for 5 min. Samples were then analysed by western blotting.

EGFP fusion constructs of rat β_{1a}-, β_{2a}-, β_3-, β_{4b}-subunits, rabbit $Ca_v2.1$ N-terminal (aa 1–98), the I–II linker (aa 361–488), the II–III linker (aa 731–1038) and the C-terminal (aa 1806–2425) were expressed in HEK293 cells and applied to the pull-down assay as previously described (*40*, *41*).

In vitro binding of the purified GST–CAST-4 and recombinant β_4-protein

Recombinant β_4-proteins [β_4(47–475)] were prepared as previously reported (*40*). Purified GST–CAST-4 fusion proteins were incubated with 50 pM purified recombinant β_4-subunits for 2 h at 4°C in phosphate-buffered saline buffer containing 0.1% Nonidet P-40 and 50 μg/ml bovine serum albumin and then incubated with glutathione-Sepharose beads for 1 h. The beads were washed twice with the phosphate-buffered saline buffer. The proteins retained on the beads were characterized by western blotting with the anti-β_4 antibody.

Western blotting

Samples were resolved using SDS-PAGE and transferred to nitrocellulose membranes (Invitrogen) or PVDF membranes (Millipore,

Temecula, CA, USA). All membranes were blocked for 1 h with blocking solution containing 5% skim milk (w/v) in TBST [20 mM Tris–Cl (pH 7.6), 140 mM NaCl, 0.1% Tween-20 (w/v)], and immunoreacted with anti-Myc (1:200), anti-HA (1:200), anti-EGFP (1:500), anti-β_4 (1:1,000), anti-CAST (1:500), anti-$Ca_v2.1$ (1:200) and anti-synaptophysin (1:1,000) antibodies. Membranes were washed and incubated for 1 h with the HRP-linked anti-mouse or anti-rabbit secondary antibody (1:5,000 for mouse, 1:2,000 for rabbit) prepared in blocking solution. Membranes were then treated with ECL solution [100 mM Tris–Cl (pH 8.5), 1.25 mM Luminol, 2.2 mM *p*-coumaric acid, 0.01% (v/v) H_2O_2] and exposed to imaging film (Kodak, New Haven, CT, USA) or a LAS-4000 image analyzer (Fujifilm, Tokyo, Japan).

Cell culture and cDNA expression in BHK cells

The BHK cell line BHK6 stably expressed the α_2/δ- and β_{4b}-subunits of VDCC as previously described (*45*). BHK6 cells were cultured in DMEM containing 10% fetal bovine serum, 30 units/ml penicillin and 30 μg/ml streptomycin. Transfection of cDNA plasmids was carried out using Effecten Transfection Reagent (Qiagen, Hilden, Germany). Cells were subjected to electrophysiological measurements 48 h after transfection.

Current recordings

Whole-cell patch-clamp recording was carried out at 22–25°C with the EPC-9 (HEKA Elektronik, Lambrecht, Pfalz, Germany) patch-clamp amplifier, as previously described (*46*). Patch pipettes (borosilicate glass capillary, 1.5 mm outer diameter, 0.87 mm inner diameter; Hilgenberg, Malsfeld, Germany) were pulled with the P-87 Flaming-Brown micropipette puller (Sutter Instrument Co., Novato, CA, USA) and fire-polished. Pipette resistance ranged from 2 to 3.5 MΩ when filled with the pipette solutions described below. The series resistance was electronically compensated to >60%, and both the leakage and the remaining capacitance were subtracted by the –P/4 method. In the experiments of activation kinetics, currents were sampled at 100 kHz after low pass filtering at 8.4 kHz (3 db), otherwise they were sampled at 20 kHz after low pass filtering at 3.0 kHz (3 db). Data were collected and analysed using the Pulse v8.77 (HEKA Elektronic). The external solution consisted of 3 mM $BaCl_2$, 155 mM tetraethylammonium chloride (TEA–Cl), 10 mM HEPES and 10 mM glucose (pH 7.4 adjusted with TEA–OH). The pipette solution consisted of 95 mM CsOH, 95 mM aspartate, 40 mM CsCl, 4 mM $MgCl_2$, 5 mM EGTA, 2 mM disodium ATP, 5 mM HEPES and 8 mM creatine phosphate (pH 7.2 adjusted with CsOH).

Voltage dependence of activation

Tail currents were elicited by repolarization to −60 mV after a 5-ms test pulse from −40 to 40 mV with 5 mV increments. Currents were sampled at 100 kHz after low pass filtering at 8.4 kHz. The amplitude of tail currents was normalized to the tail current amplitude obtained with a test pulse of 40 mV. Mean values were plotted against test pulse potentials and fitted to the Boltzmann equation: $n(V_m) = 1/\{1 + \exp[(V_{0.5} - V_m)/k]\}$, where V_m is membrane potential, $V_{0.5}$ is the potential that gives a half-value of conductance and k is the slope factor.

Voltage dependence of inactivation

The voltage dependence of VDCC inactivation (inactivation curve) was determined by a double-pulse protocol with a 2-s inactivation pulse (conditional pulse) from −100 to 20 mV (10 mV increments) and a 20-ms test pulse to 5 mV following 10 ms interpulse interval at the holding potential of −100 mV. Current amplitudes elicited by the test pulses were normalized to those after the 2-s conditional pulse to −100 mV. Mean values were plotted against the potentials of the conditional pulse and fitted to the Boltzmann equation as described above.

Statistical analyses

All data are expressed as means ± SEM. We accumulated the data for each condition from at least three independent experiments. Statistical significance was evaluated with an ANOVA followed by Tukey–Kramer test. $P < 0.05$ was considered statistically significant.

Results

Direct interaction of CAST with the VDCC β_4-subunit

Nishimune *et al*. have recently reported that CAST or the family member, ELKS, interacts with VDCC β-subunits using recombinant HEK293 cell lysates (*47*, *48*). To examine the interaction of the active zone protein CAST with VDCC complexes in native system, we used the immunoprecipitation assay on brain samples. First, we immunoprecipitated β_4-subunit with its antibody from the detergent extract of the mouse brain synaptosomal fraction. Consistent with the previous report that β_1-subunit directly binds to CAST in a heterologous expression system of HEK293 cells (*47*), CAST was coimmunoprecipitated with the β_4-subunit, but the synaptic vesicle protein synaptophysin was not (Fig. 1A). Moreover, when the immunoprecipitation assay was performed on the brain extract of lethargic mice, which carry a mutated form of the *VDCC β4* gene (*49*), CAST was not immunoprecipitated (data not shown). Accordingly, these results suggest that CAST interacts with β_4-subunit in the intact brain.

We further examined the mode of binding between CAST and the VDCC β_4-subunit using pull-down assays with various GST-tagged CAST fragments (Fig. 1B). The extract of HEK293 cells expressing Myc-VDCC β_{4b} was incubated with glutathione-Sepharose beads containing various GST–CAST fusion proteins. Myc-VDCC β_{4b} bound to GST–CAST-1 containing the first coiled-coil (CC) domain and GST–CAST-4 containing the last CC domain and a unique C-terminal amino acid (Ile–Trp–Ala) called IWA motif, but not to the other GST fusion proteins (Fig. 1C). Under the same conditions, RIM1 and Bassoon bound to GST–CAST-4 and GST–CAST-2, respectively (Fig. 1C) (*2*, *10*). The IWA motif is essential for CAST to bind the PDZ domain of RIM1 (*2*, *3*). Thus, HA-RIM1 did not bind to GST–CAST-4ΔIWA, whereas Myc-VDCC β_{4b} bound to it (Fig. 1D).

Next, we examined the ability of other β-subunits (β_{1a}, β_{2a} and β_3) to bind to CAST. GST pull-down assays revealed that not only β_{4b}-subunit but also other β-subunits bound to GST–CAST-4 (Fig. 2A). Interestingly, GST–CAST-4 had a higher binding potency to β_{4b}-subunit, the brain-type β-subunit, compared with the skeletal muscle-type β_{1a}-subunit, the cardiac muscle type β_{2a}-subunit and the brain-type β_3-subunit (*50*). Importantly, the purified preparation of recombinant β_4-subunit [β_4(47–475)] (*40*) was also pulled-down by the purified GST–CAST-4 (Fig. 2B). These results suggest that CAST forms a protein complex with VDCCs through direct interactions with VDCC β-subunits.

Complex formation of CAST with VDCC subunits in the brain

We examined the binding of CAST with VDCC subunits by pull-down assays using brain lysates. To this end, we prepared the brain fraction containing VDCC complexes (*41*) and incubated the extract with glutathione-Sepharose beads containing various

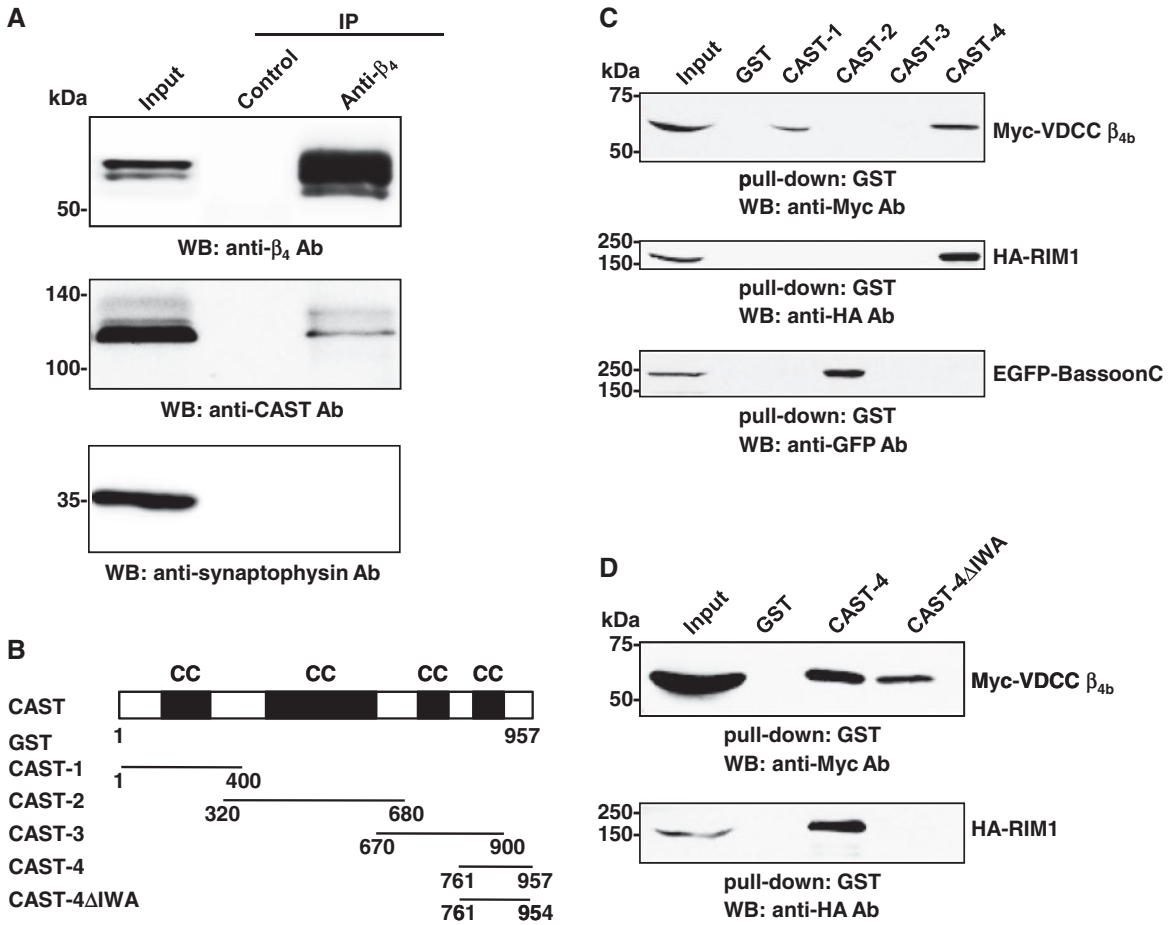

Fig. 1 Interaction of CAST and VDCC β_4-subunit. (**A**) Coimmunoprecipitation of CAST with VDCC β_4. The detergent extract of the mouse brain synaptosomal fraction was subjected to immunoprecipitation with the anti-β_4 antibody. The immunoprecipitate was analysed by western blotting using antibodies against indicated proteins: anti-β_4, anti-CAST and anti-synaptophysin. Ab, antibody; IP, immunoprecipitation; WB, western blotting. (**B**) GST fusion constructs of CAST. CAST-1 to -4 includes at least one coiled-coil domain (CC). And CAST-4ΔIWA lacks the C-terminal three amino acid (Ile–Trp–Ala) called IWA motif. The numbers indicate amino acid positions. (**C**) Direct binding of VDCC β_{4b}-subunit to CAST. The extract of HEK293 cells expressing Myc-VDCC β_{4b}, HA-RIM1 or EGFP-BassoonC was then incubated with the beads which are conjugated with various regions of CAST-1 to -4 as well as GST alone. Proteins that bound to the beads were analysed by western blotting using the anti-Myc, anti-HA or anti-GFP antibodies. Input contains 8.0% (for VDCC and RIM1) and 32% (for BassoonC) of the extract was used for this assay. (**D**) Distinct CAST-binding regions for RIM1 and VDCC β_{4b}-subunit. The extract of HEK293 cells expressing Myc-VDCC β_{4b} or HA-RIM1 was incubated with the beads immobilized with CAST-4, CAST-4ΔIWA or GST alone. HA-RIM1 only bound to the CAST-4, while Myc-VDCC β_{4b} bound both CAST-4 and CAST-4ΔIWA. Input contains 16% (for VDCC) and 12% (for RIM) of the extract used for this assay.

GST–CAST proteins (Fig. 1B). Both VDCC α_1- and β_4-subunits could be detected by those subunit-specific antibodies binding to GST–CAST-4 (Fig. 3). However, in contrast to the result in Fig. 1C, we did not detect binding of VDCC β_4-subunit to GST–CAST-1 in this brain lysate system (Fig. 3B).

Interaction of CAST with the VDCC α_1-subunit

In *Drosophila*, the CAST homologue Brp has been shown to interact with the C-terminal region of VDCC α_1-subunits and to regulate its clustering at the active zone (*51*). In vertebrate, we found a complex formation of VDCC α_1-subunit and CAST (Fig. 3). Therefore, we examined the direct interaction between CAST and VDCC α_1-subunit (Fig. 4). To this end, we prepared fragments of the N-terminal (aa 1–98), I–II linker (aa 361–488), II–III linker (aa 731–1038) and C-terminal (aa 1806–2425) regions of the VDCC α_1-subunit, $Ca_v2.1$. All these regions are located at the cytoplasmic side of the plasma membrane and thus might bind to CAST directly. Extracts of EGFP-tagged VDCC α_1 fragments or that of VDCC β_4-subunit from HEK293 cells revealed equal expression at the protein level (Fig. 4B). Consistent with the results in Figs. 1 and 3, pull-down assay using GST–CAST-4 indicated the direct interaction of EGFP-VDCC β_4-subunit to CAST. For the α_1-subunit, not C-terminal but II–III linker of $Ca_v2.1$ interacted with GST–CAST-4 (Fig. 4A). Chen *et al.* have also reported that the C-terminal region of the VDCC α_1-subunit does not coimmunoprecipitate with CAST in a heterologous expression system of HEK cells (*47*). These results indicate that interaction regions of α_1-subunit for CAST are different between *Drosophila* and mice. In addition, the interaction of II–III linker with GST–CAST-4 was much weaker than that of β_4-subunit. Therefore, in mammalian systems, we conclude that CAST has

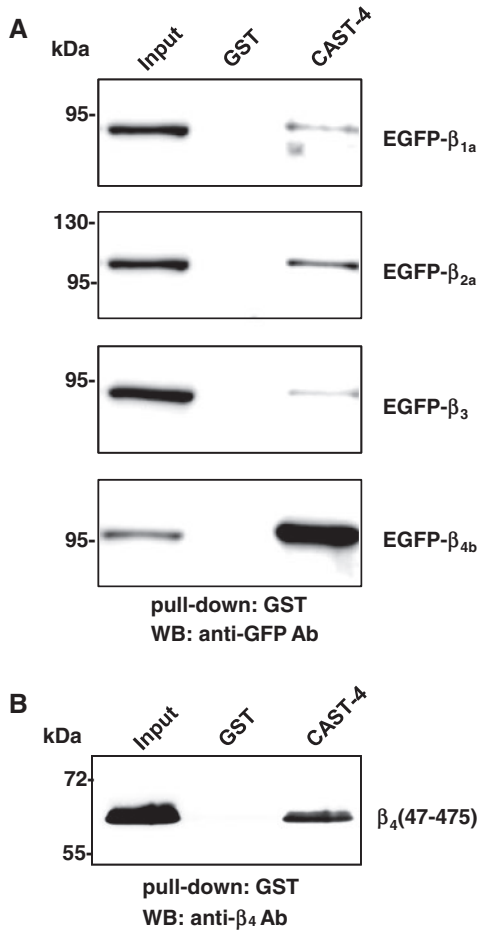

Fig. 2 Direct binding of CAST with VDCC β-subunits. (**A**) GST-pull-down assay of β-subunits (β_{1a}, β_{2a}, β_3 and β_{4b}) with GST–CAST-4. GST–CAST-4 bound glutathione-Sepharose beads were incubated with cell lysates obtained from EGFP-β-transfected HEK293 cells. Bound proteins were analysed by western blotting using anti-GFP antibody. (**B**) *In vitro* association between the purified GST–CAST-4 and recombinant β_4-subunit [β_4(47–475)]. GST–CAST-4 incubated with β_4-subunit was captured by glutathione-Sepharose beads. Captured β_4-proteins were examined by western blotting.

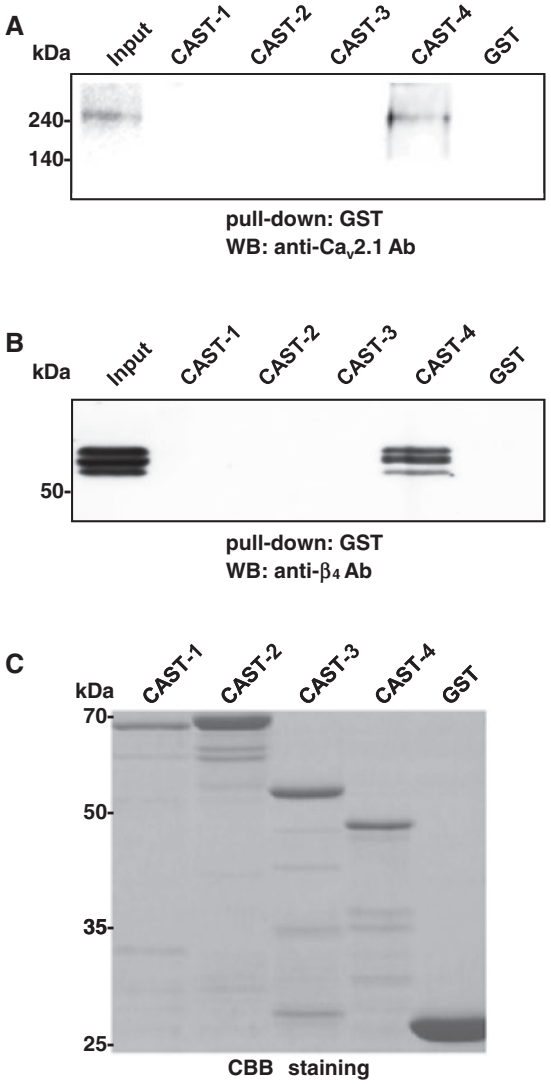

Fig. 3 Complex formation of CAST with VDCCs through the β_4-subunit. (**A** and **B**) The GST fusion proteins containing various CAST regions (Fig. 1B) as well as GST alone were immobilized on glutathione-Sepharose beads. The detergent extract of the mouse brain synaptosomal fraction was then incubated with the beads, and proteins that bound to the beads were analysed by western blotting using the indicated antibodies. The endogenous VDCC α_1-subunit (anti-$Ca_v2.1$) and VDCC β_4-subunit were pull-downed by CAST-4. (**C**) Coomassie brilliant blue (CBB) staining of loaded GST fusion proteins.

the potency to form a complex with VDCCs mainly with β_4-subunit through its direct interaction.

Functional effects of CAST on P/Q-type VDCC currents

Biochemical and molecular biological approaches have revealed the physical and functional interactions of VDCCs with synaptic proteins such as syntaxin, SNAP-25, synaptotagmin and RIMs (*21–24*, *30*, *40–43*). To obtain further insight into the functional linkage between the active zone proteins and VDCCs, we elucidated the physiological significance of the direct interaction between CAST and the VDCC β-subunits. First, we examined whole-cell Ba^{2+} currents through recombinant P/Q-type VDCC expressed as $\alpha_1 \cdot \alpha_2/\delta \cdot \beta$ complexes containing the BI-2 variant of $Ca_v2.1$ (*31*) and β_{4b}-subunit in BHK cells. We focused on P/Q-type VDCC in this study, because P/Q-type VDCC is known to contribute to neurotransmitter release at presynapse (*17*, *18*). Fig. 5 shows Ca^{2+}-channel currents and their current–voltage (I–V) relationships in the BHK cells in the presence or absence of full-length CAST. Ba^{2+} currents were elicited with 30 ms depolarizing pulses from a holding potential ($V_h = -100$ mV) to test potentials from −40 to 40 mV with increments of 10 mV in a 3 mM Ba^{2+} solution. We found that CAST slightly shifted the I–V relationship in the hyperpolarizing direction by ~5 mV without affecting the current density (Fig. 5 and Table I). These results suggest that CAST may regulate the opening of VDCCs.

Effects of CAST on activation properties of VDCC currents

To clarify this hypothesis, we next examined the effect of CAST on the activation of the P/Q-type VDCC.

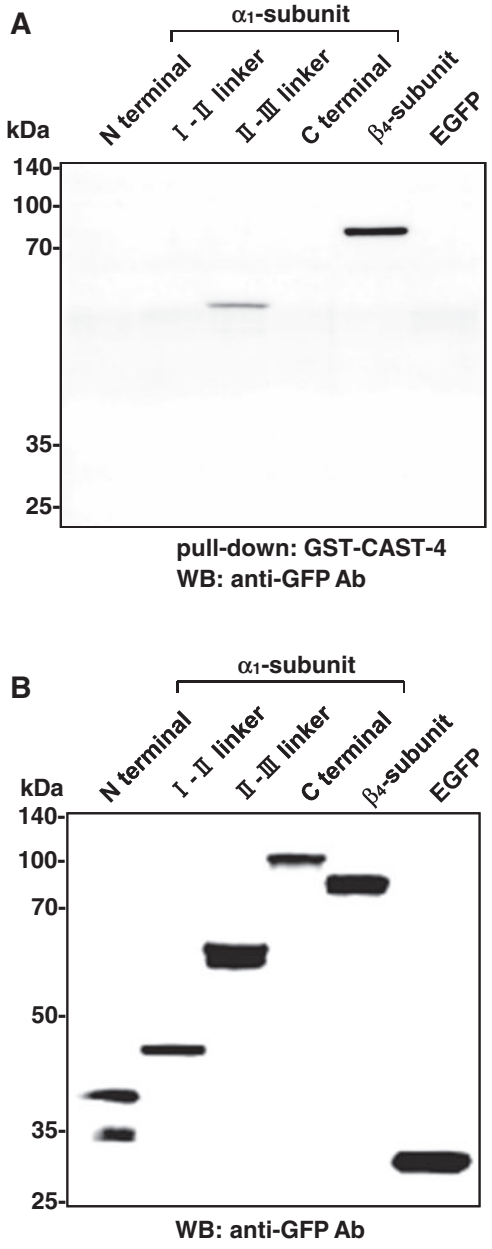

Fig. 4 Interaction of the VDCC α_1-subunit with the C-terminal region of CAST. (**A**) The extracts of HEK293 cells expressing the indicated EGFP-tagged fragments of the α_1-subunit, full-length β_{4b}-subunit and control EGFP were incubated with the beads on which GST–CAST-4 was immobilized. Proteins were analysed by western blotting using the anti-GFP antibody. (**B**) Expression and input of EGFP-tagged fragments of the α_1-subunit and full-length the β_{4b}-subunit were assessed by western blotting.

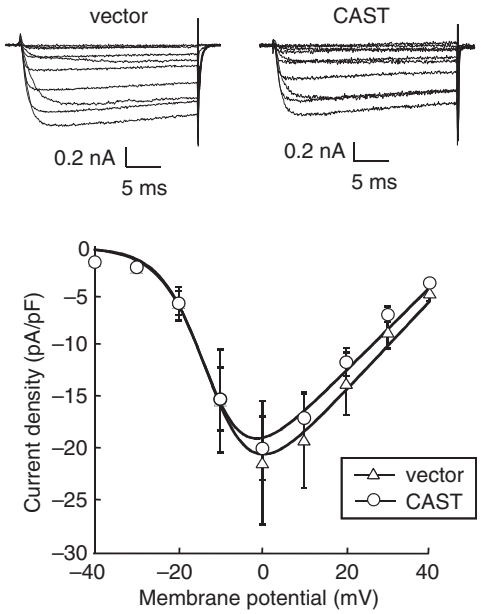

Fig. 5 Effects of CAST on the *I–V* relationships of P/Q-type Ca^{2+} channel. Voltage-dependent activation of P/Q-type Ca^{2+} channel current in BHK cells expressing α_2/δ- and β_{4b}-subunit. Representative Ba^{2+} currents evoked by 30 ms depolarizing pulses from −40 to 40 mV (upper) with 10 mV increments from a V_h of −100 mV, and the current density–voltage (*I–V*) relationship (lower). In the presence of CAST, the *I–V* relationship was slightly shifted to the hyperpolarization as compared to the vector alone. Data points are mean ± SEM.

The activation curves, which were obtained by fitting the peak amplitude of tail currents with the Boltzmann equation, showed different voltage dependence with CAST coexpression (Fig. 6A). The voltage dependence of activation was shifted in the hyperpolarizing direction, and the midpoints of the activation curves ($V_{0.5}$) were -10.8 ± 1.0 and -5.0 ± 1.3 mV in the presence and absence of CAST, respectively (Table I). Interestingly, in the cells expressing β_1-subunit instead of β_4-subunit, the leftward shift of the voltage-dependent activation was not observed (data not shown). CAST also changed the slope factor (k) from 7.0 ± 0.4 to 5.5 ± 0.1 mV (Table I) and modulated the activation kinetics of P/Q-type VDCCs (Fig. 6B). The time constant ($\tau_{activation}$) obtained by fitting the activation time course of inward currents with a single exponential was 'bell-shaped' when plotted against different voltages (Fig. 6B). CAST decelerated the activation kinetics at membrane potentials of −25, −10 and −5 mV. Thus, in CAST-containing synapse, neurotransmission may occur at the hyperpolarizing potentials at which other synapses are not activated. Decreased activation rate of the channels may prevent Ca^{2+} overload at the hyperpolarizing potentials.

Effects of CAST on inactivation properties of VDCC currents

We examined the effect of CAST on the inactivation properties of the P/Q-type VDCC. The voltage dependence of inactivation was determined by the use of 2 s prepulses to a series of different potentials followed by the test pulse to 5 mV. Peak current amplitudes were normalized to the peak current amplitude induced by the test pulse from a prepulse potential of −100 mV and were plotted against the prepulse potentials. CAST did not affect the voltage dependence of inactivation (Fig. 7). The estimated half-inactivation potential and the slope factor of the inactivation curves fitted by the Boltzmann equation were -50.6 ± 1.7 and -8.5 ± 0.5 mV in the presence of CAST, and -48.1 ± 2.1 and -8.5 ± 0.3 mV in the absence of CAST, respectively (Table I).

Table I. Effects of CAST on current density, activation and inactivation of $Ca_v2.1$ channels in BHK cells expressing α_2/δ- and β_{4b}-subunits[a].

		Activation parameters		Inactivation parameters	
	Current density (pA/pF)[b]	$V_{0.5}$ (mV)	k (mV)	$V_{0.5}$ (mV)	k (mV)
Vector	−20.6 ± 5.1 (7)[c]	−5.0 ± 1.3 (5)	7.0 ± 0.4 (5)	−48.1 ± 2.1 (3)	−8.5 ± 3 (3)
CAST	−19.5 ± 3.1 (14)	−10.8 ± 1.0 (8)**	5.5 ± 0.1 (8)**	−50.6 ± 1.7 (7)	−8.5 ± 0.5 (7)

[a]**$P<0.01$ vs. vector
[b]Ba^{2+} currents evoked by depolarizing pulse to 0 mV from a V_h (−100 mV) were divided by capacitances.
[c]Number of cells analysed is indicated in the parenthesis.

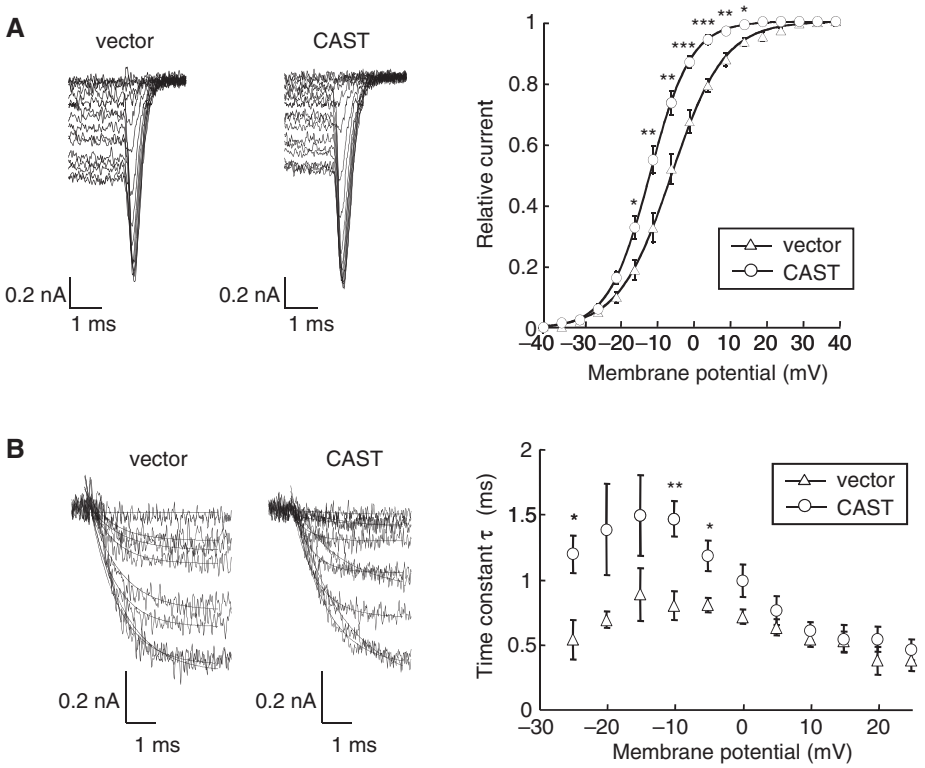

Fig. 6 Effects of CAST on the activation properties of P/Q-type Ca^{2+} channel. (**A**) Superimposed tail current elicited by repolarization to −60 mV after the 5 ms test pulse from −40 to 40 mV with increments of 5 mV (left), and normalized tail current were plotted against test-pulse potentials (right). The Boltzman fit to each plots represented the hyperpolarization shift of activation property of P/Q-type Ca^{2+} channel in the presence of CAST. (**B**) Activation kinetics of P/Q-type Ca^{2+} channel currents. (Left) Families of Ba^{2+} currents and the single exponential fit on their activation phases. Currents were evoked by 5 ms step depolarizations from −25 to 25 mV from the holding potential ($V_h = -100$ mV). (Right) Comparison of the activation time constant ($\tau_{activation}$). The activation time constant (τ) obtained from the single exponential fit was significantly increased in the presence of CAST at −25, −10 and −5 mV membrane potential. *$P<0.05$, **$P<0.01$ and ***$P<0.001$. Data points are mean ± SEM.

Discussion

In the present study, we have shown that the active zone protein CAST binds the VDCC β_4-subunit directly and forms a protein complex with VDCCs at the presynaptic active zone, modifying the opening of VDCCs. Pull-down assays and immunoprecipitation experiments have also identified their direct interaction which involves at least the C-terminal region of CAST. Therefore, our results indicate that CAST regulates neurotransmitter release by modifying the opening of VDCCs through the physical association with the VDCC β-subunit.

CAST has been shown to be localized at the active zone by immunoelectron microscopy (*2*, *4*) and binds with a number of synaptic proteins, mainly cytoplasmic at the active zone proteins (*10*). The results in our study demonstrate that CAST interacts directly with the VDCC β_4-subunit (Fig. 1) in addition to the active zone proteins Bassoon, Piccolo and RIM1 (*10*). The VDCC β_4-subunit bound to the N- and C-terminal regions of CAST (GST–CAST-1 and GST–CAST-4; Fig. 1C), which are distinct from the binding regions for Bassoon, Piccolo and RIM1 (*2*, *10*). Intriguingly, the VDCC β_4-subunit bound to GST–CAST-4ΔIWA, to which RIM1 does not bind (Fig. 1D). These distinct CAST-binding regions for the VDCC β_4-subunit and RIM1 would be advantageous for regulating VDCC activity at the molecular level. One scenario may be that CAST recruits RIM1 at the active zone and

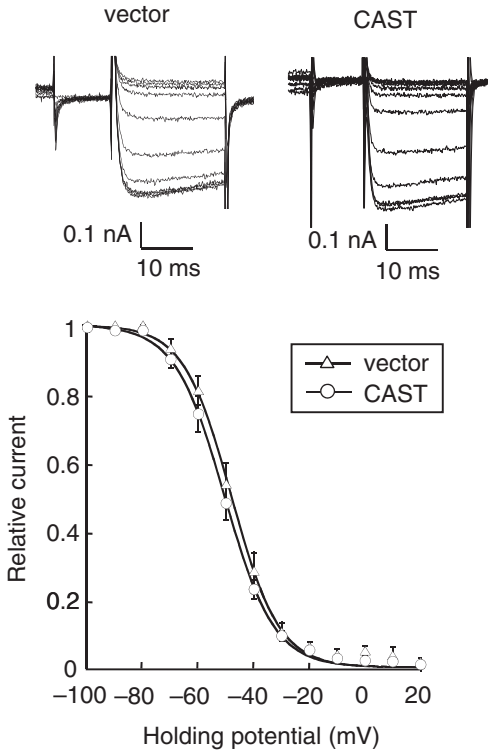

Fig. 7 Effects of CAST on the inactivation properties of P/Q-type Ca^{2+} channel. (Upper) Ba^{2+} currents were evoked by a 20 ms test pulse to 5 mV after the 10 ms repolarization to holding potential (−100 mV) following a 2 s inactivation pulse (conditional pulse) from −100 to 20 mV with increments of 10 mV. (Lower) Normalized test pulse currents were plotted against conditional pulse potentials and fitted with the Boltzman equation. The inactivation curve was not significantly different with or without CAST. Data points are mean ± SEM.

RIM1 in turn bind to the VDCC β_4-subunit on CAST, suggesting that CAST may serve as a platform for the VDCC β_4-subunit–RIM1 interaction. Indeed, using primary rat hippocampal neuron cultures (*2*) and CAST/ERC2 knockout mice (*16*), CAST has been suggested to be involved in anchoring RIM1 to the active zone. Another possibility is that RIM1 competes with β_4-subunit for the binding to CAST. Whether CAST recruits the VDCC β_4-subunit in addition to RIM1 has not been examined; however, elucidation of the involvement of CAST in anchoring the VDCC β_4-subunit to the active zone will shed new light on the molecular mechanisms responsible for direct and functional interactions between active zone proteins and VDCCs.

As mentioned above and in Fig. 1, the VDCC β_4-subunit bound to GST–CAST-4 as well as to GST–CAST-1, but the pull-down assay using the mouse brain lysate showed that the VDCC β_4-subunit bound only to GST–CAST-4 (Fig. 3B). At present, we cannot explain this difference, but we speculate that there is a protein that binds the N-terminal region of CAST (CAST-1) in the brain lysate, which may interfere with the binding of the VDCC β_4-subunit to the region.

Consistent with previous observations (*47*), our present results demonstrate that CAST does not interact directly with the C-terminal region of VDCC α_1-subunits (Fig. 4). In this study, we have revealed that the II–III linker of α_1-subunits interacts with CAST, but the interaction appears to be weaker compared with that of the β_4-subunit. However, in *Drosophila*, Brp, the only homologue of the ELKS/CAST family, has been shown to interact directly with the C-terminal region of P/Q-type VDCC α_1-subunit homologue, Cacophony (*51*). Brp mutants and knockdown studies have shown that the clustering of Cacophony was significantly reduced at the active zones. Presently, we cannot explain the discrepancy in the binding of CAST and the VDCC α_1-subunit, but we speculate that there is a different mechanism for clustering VDCCs at the active zone of mice and flies. Indeed, the active zone proteins Bassoon and Piccolo are not conserved in invertebrates such as *C. elegans* and *Drosophila*. Recently, Chen *et al*. have also reported that Bassoon binds directly to the VDCC β_4-subunit (*47*). In addition, unlike *Drosophila*, the deletion of the *C. elegans* ELKS/CAST homologue appeared to have no effect on the assembly of the active zone (*52*). Thus, we suggest that the clustering of VDCCs at the active zone and its assembly are much more complicated than envisaged.

β_3- and β_4-subunits are generally known as brain-type VDCC β-subunits. However, these distributions are different in nervous systems (*50*, *53*). The expression of β_3-subunit is highest in the olfactory bulb and habenula. Moderate β_3-subunit signals are detected in the cortex, hippocampus, basal ganglia, nucleus interpeduncularis, superior colliculus and cerebellum. In contrast, the expression of β_4-subunit is highest in the cerebellum and is not detected in habenula. Moderate β_4-subunit signals are found in the olfactory bulb, cortex, hippocampus, basal ganglia and inferior colliculus. In addition, subunit compositions of VDCCs are also different in brains. Biochemical assay reveals that the most prevalent partner of $Ca_v2.2$ (N-type) is β_3-subunit and that of $Ca_v2.1$ (P/Q-type) is β_4-subunit (*50*, *54*, *55*). In this study, we revealed that CAST preferentially interacts with β_4-subunit among β-subunits (β_1, β_2, β_3 and β_4). Thus, CAST may mainly scaffold and functionally modulate P/Q-type VDCCs at β_4-containing synapses in the brain.

The presynaptic VDCCs, N-type and P/Q-type Ca^{2+} channels, are subject to functional modulation by interaction with synaptic proteins that finely tune Ca^{2+} entry into nerve terminals. Most synaptic proteins affect the inactivation properties of VDCCs. Syntaxin or SNAP-25 binds to the II–III linker of the α_1-subunit to decrease channel availability with a hyperpolarizing shift in the voltage dependence of inactivation of transiently expressed (*22–24*, *27*) and native Ca^{2+} channels (*56*). By binding to the β-subunit (*40*, *41*) or the C-terminal of the α_1-subunit (*42*), RIM1 sustains Ca^{2+} influx through the inhibition of voltage-dependent inactivation of VDCCs (*40*, *41*, *43*). In contrast, Ca^{2+}-binding protein 1 (CaBP1), which binds to the C-terminal of the α_1-subunit, modulates activation properties. CaBP1 induces a depolarizing shift in the voltage dependence of activation of

VDCCs, thus inhibiting channel activity by antagonizing channel opening (*57*). In the present study, we reveal that CAST modulates activation properties. Interestingly, CAST binds to the β-subunit, but not the α_1-subunit, and shifts voltage dependence of activation towards the hyperpolarizing direction. Thus, CAST may enhance the β-subunit action on Ca^{2+} channel properties, because the β-subunits shift the voltage dependence of activation to hyperpolarizing direction (*33*, *34*, *50*).

In summary, we show here that the direct binding of CAST and the VDCC β_4-subunit regulates the opening of the functional VDCC complex. Notably, this is the first report to show that the activation of VDCC is directly affected by an active zone protein. Further biochemical analyses focused on the potential property of CAST to anchor RIMs to the active zone (*2*, *16*) would shed new light on our understanding of the mode of functional complex formation.

Acknowledgements

The authors thank M. Yagi for expert experiments and S. Mochida for helpful comments and discussion.

Funding

This work was supported by a grant-in-aid for Scientific Research (B) (22300120 to T.O.) and for Scientific Research on Priority Areas (20022021 to S.K.) from the Ministry of Education, Culture, Sports, Science and Technology of Japan and by Takeda Science Foundation (to T.O.).

Conflict of interest

None declared.

References

1. Landis, D.M., Hall, A.K., Weinstein, L.A., and Reese, T.S. (1988) The organization of cytoplasm at the presynaptic active zone of a central nervous system synapse. *Neuron* **1**, 201–209
2. Ohtsuka, T., Takao-Rikitsu, E., Inoue, E., Inoue, M., Takeuchi, M., Matsubara, K., Deguchi-Tawarada, M., Satoh, K., Morimoto, K., Nakanishi, H., and Takai, Y. (2002) CAST: a novel protein of the cytomatrix at the active zone of synapses that forms a ternary complex with RIM1 and Munc13-1. *J. Cell. Biol.* **158**, 577–590
3. Wang, Y., Liu, X., Biederer, T., and Südhof, T.C. (2002) A family of RIM-binding proteins regulated by alternative splicing: Implications for the genesis of synaptic active zones. *Proc. Natl. Acad. Sci. U.S.A.* **99**, 14464–14469
4. Deguchi-Tawarada, M., Inoue, E., Takao-Rikitsu, E., Inoue, M., Ohtsuka, T., and Takai, Y. (2004) CAST2: identification and characterization of a protein structurally related to the presynaptic cytomatrix protein CAST. *Genes Cells* **9**, 15–23
5. tom Dieck, S., Sanmartí-Vila, L., Langnaese, K., Richter, K., Kindler, S., Soyke, A., Wex, H., Smalla, K.H., Kämpf, U., Fränzer, J.T., Stumm, M., Garner, C.C., and Gundelfinger, E.D. (1998) Bassoon, a novel zinc-finger CAG/glutamine-repeat protein selectively localized at the active zone of presynaptic nerve terminals. *J. Cell Biol.* **142**, 499–509
6. Wang, X., Kibschull, M., Laue, M.M., Lichte, B., Petrasch-Parwez, E., and Kilimann, M.W. (1999) Aczonin, a 550-kD putative scaffolding protein of presynaptic active zones, shares homology regions with Rim and Bassoon and binds profilin. *J. Cell. Biol.* **147**, 151–162
7. Fenster, S.D., Chung, W.J., Zhai, R., Cases-Langhoff, C., Voss, B., Garner, A.M., Kämpf, U., Kindler, S., Gundelfinger, E.D., and Garner, C.C. (2000) Piccolo, a presynaptic zinc finger protein structurally related to bassoon. *Neuron* **25**, 203–214
8. Brose, N., Hofmann, K., Hata, Y., and Südhof, T.C. (1995) Mammalian homologues of *Caenorhabditis elegans unc-13* gene define novel family of C_2-domain proteins. *J. Biol. Chem.* **270**, 25273–25280
9. Wang, Y., Okamoto, M., Schmitz, F., Hofmann, K., and Südhof, T.C. (1997) Rim is a putative Rab3 effector in regulating synaptic-vesicle fusion. *Nature* **388**, 593–598
10. Takao-Rikitsu, E., Mochida, S., Inoue, E., Deguchi-Tawarada, M., Inoue, M., Ohtsuka, T., and Takai, Y. (2004) Physical and functional interaction of the active zone proteins, CAST, RIM1, and Bassoon, in neurotransmitter release. *J. Cell Biol.* **164**, 301–311
11. Hida, Y. and Ohtsuka, T. (2010) CAST and ELKS proteins: structural and functional determinants of the presynaptic active zone. *J. Biochem.* **148**, 131–137
12. Kittel, R.J., Wichmann, C., Rasse, T.M., Fouquet, W., Schmidt, M., Schmid, A., Wagh, D.A., Pawlu, C., Kellner, R.R., Willig, K.I., Hell, S.W., Buchner, E., Heckmann, M., and Sigrist, S.J. (2006) Bruchpilot promotes active zone assembly, Ca^{2+} channel clustering, and vesicle release. *Science* **312**, 1051–1054
13. Wagh, D.A., Rasse, T.M., Asan, E., Hofbauer, A., Schwenkert, I., Dürrbeck, H., Buchner, S., Dabauvalle, M.C., Schmidt, M., Qin, G., Wichmann, C., Kittel, R., Sigrist, S.J., and Buchner, E. (2006) Bruchpilot, a protein with homology to ELKS/CAST, is required for structural integrity and function of synaptic active zones in *Drosophila*. *Neuron* **49**, 833–844
14. Inoue, E., Deguchi-Tawarada, M., Takao-Rikitsu, E., Inoue, M., Kitajima, I., Ohtsuka, T., and Takai, Y. (2006) ELKS, a protein structurally related to the active zone protein CAST, is involved in Ca^{2+}-dependent exocytosis from PC12 cells. *Genes Cells* **11**, 659–672
15. Ohara-Imaizumi, M., Ohtsuka, T., Matsushima, S., Akimoto, Y., Nishiwaki, C., Nakamichi, Y., Kikuta, T., Nagai, S., Kawakami, H., Watanabe, T., and Nagamatsu, S. (2005) ELKS, a protein structurally related to the active zone-associated protein CAST, is expressed in pancreatic beta cells and functions in insulin exocytosis: interaction of ELKS with exocytotic machinery analyzed by total internal reflection fluorescence microscopy. *Mol. Biol. Cell.* **16**, 3289–3300
16. Kaeser, P.S., Deng, L., Chávez, A.E., Liu, X., Castillo, P.E., and Südhof, T.C. (2009) ELKS2α/CAST deletion selectively increases neurotransmitter release at inhibitory synapses. *Neuron* **64**, 227–239
17. Takahashi, T. and Momiyama, A. (1993) Different types of calcium channels mediate central synaptic transmission. *Nature* **366**, 156–158
18. Wheeler, D.B., Randall, A., and Tsien, R.W. (1994) Roles of N-type and Q-type Ca^{2+} channels in supporting hippocampal synaptic transmission. *Science* **264**, 107–111
19. Catterall, W.A. (1998) Structure and function of neuronal Ca^{2+} channels and their role in neurotransmitter release. *Cell Calcium* **24**, 307–323
20. Ertel, E.A., Campbell, K.P., Harpold, M.M., Hofmann, F., Mori, Y., Perez-Reyes, E., Schwartz, A., Snutch,

T.P., Tanabe, T., Birnbaumer, L., Tsien, R.W., and Catterall, W.A. (2000) Nomenclature of voltage-gated calcium channels. *Neuron* **25**, 533–535

21. Sheng, Z.H., Rettig, J., Takahashi, M., and Catterall, W.A. (1994) Identification of a syntaxin-binding site of N-type calcium channels. *Neuron* **13**, 1303–1313
22. Bezprozvanny, I., Scheller, R.H., and Tsien, R.W. (1995) Functional impact of syntaxin on gating of N-type and Q-type calcium channels. *Nature* **378**, 623–626
23. Wister, O., Bennett, M.K., and Atlas, D. (1996) Functional interaction of syntaxin and SNAP-25 with voltage-sensitive L- and N-type Ca^{2+} channels. *EMBO J.* **15**, 4100–4110
24. Zhong, H., Yokoyama, C.T., Scheuer, T., and Catterall, W.A. (1999) Reciprocal regulation of P/Q-type Ca^{2+} channels by SNAP-25, syntaxin and synaptotagmin. *Nat. Neurosci.* **2**, 939–941
25. Maximov, A., Südhof, T.C., and Bezprozvanny, I. (1999) Association of neuronal calcium channels with modular adaptor proteins. *J. Biol. Chem.* **274**, 24453–24456
26. Maximov, A. and Bezprozvanny, I. (2002) Synaptic targeting of N-type calcium channels in hippocampal neurons. *J. Neurosci.* **22**, 6939–6952
27. Spafford, J.D. and Zamponi, G.W. (2003) Functional interactions between presynaptic calcium channels and the neurotransmitter release machinery. *Curr. Opin. Neurobiol.* **13**, 308–314
28. Nishimune, H., Sanes, J.R., and Carlson, S.S. (2004) A synaptic laminin-calcium channel interaction organizes active zones in motor nerve terminals. *Nature* **432**, 580–587
29. Kang, M.G., Chen, C.C., Wakamori, M., Hara, Y., Mori, Y., and Campbell, K.P. (2006) A functional AMPA receptor-calcium channel complex in the postsynaptic membrane. *Proc. Natl. Acad. Sci. U.S.A.* **103**, 5561–5566
30. Watanabe, H., Yamashita, T., Saitoh, N., Kiyonaka, S., Iwamatsu, A., Campbell, K.P., Mori, Y., and Takahashi, T. (2010) Involvement of Ca^{2+} channel synprint site in synaptic vesicle endocytosis. *J. Neurosci.* **30**, 655–660
31. Mori, Y., Friedrich, T., Kim, M.S., Mikami, A., Nakai, J., Ruth, P., Bosse, E., Hofmann, F., Flockerzi, V., Furuichi, T., Mikoshiba, K., Imoto, K., Tanabe, T., and Numa, S. (1991) Primary structure and functional expression from complementary DNA of a brain calcium channel. *Nature* **350**, 398–402
32. Bichet, D., Cornet, V., Geib, S., Carlier, E., Volsen, S., Hoshi, T., Mori, Y., and De Waard, M. (2000) The I-II loop of the Ca^{2+} channel α_1 subunit contains an endoplasmic reticulum retention signal antagonized by the β subunit. *Neuron* **25**, 177–190
33. Varadi, G., Lory, P., Schultz, D., Varadi, M., and Schwartz, A. (1991) Acceleration of activation and inactivation by the β subunit of the skeletal muscle calcium channel. *Nature* **352**, 159–162
34. Lacerda, A.E., Kim, H.S., Ruth, P., Perez-Reyes, E., Flockerzi, V., Hofmann, F., Birnbaumer, L., and Brown, A.M. (1991) Normalization of current kinetics by interaction between the α_1 and β subunits of the skeletal muscle dihydropyridine-sensitive Ca^{2+} channel. *Nature* **352**, 527–530
35. Béguin, P., Nagashima, K., Gonoi, T., Shibasaki, T., Takahashi, K., Kashima, Y., Ozaki, N., Geering, K., Iwanaga, T., and Seino, S. (2001) Regulation of Ca^{2+} channel expression at the cell surface by the small G-protein kir/Gem. *Nature* **411**, 701–706
36. Hibino, H., Pironkova, R., Onwumere, O., Rousset, M., Charnet, P., Hudspeth, A.J., and Lesage, F. (2003) Direct interaction with a nuclear protein and regulation of gene silencing by a variant of the Ca^{2+}-channel β_4 subunit. *Proc. Natl. Acad. Sci. U.S.A.* **100**, 307–312
37. Vendel, A.C., Terry, M.D., Striegel, A.R., Iverson, N.M., Leuranguer, V., Rithner, C.D., Lyons, B.A., Pickard, G.E., Tobet, S.A., and Horne, W.A. (2006) Alternative splicing of the voltage-gated Ca^{2+} channel β_4 subunit creates a uniquely folded N-terminal protein binding domain with cell-specific expression in the cerebellar cortex. *J. Neurosci.* **26**, 2635–2644
38. Gonzalez-Gutierrez, G., Miranda-Laferte, E., Neely, A., and Hidalgo, P. (2007) The Src homology 3 domain of the β-subunit of voltage-gated calcium channels promotes endocytosis via dynamin interaction. *J. Biol. Chem.* **282**, 2156–2162
39. Zhang, Y., Yamada, Y., Fan, M., Bangaru, S.D., Lin, B., and Yang, J. (2010) The β subunit of voltage-gated Ca^{2+} channels interacts with and regulates the activity of a novel isoform of Pax6. *J. Biol. Chem.* **285**, 2527–2536
40. Kiyonaka, S., Wakamori, M., Miki, T., Uriu, Y., Nonaka, M., Bito, H., Beedle, A.M., Mori, E., Hara, Y., De Waard, M., Kanagawa, M., Itakura, M., Takahashi, M., Campbell, K.P., and Mori, Y. (2007) RIM1 confers sustained activity and neurotransmitter vesicle anchoring to presynaptic Ca^{2+} channels. *Nat. Neurosci.* **10**, 691–701
41. Uriu, Y., Kiyonaka, S., Miki, T., Yagi, M., Akiyama, S., Mori, E., Nakao, A., Beedle, A.M., Campbell, K.P., Wakamori, M., and Mori, Y. (2010) Rab3-interacting molecule γ isoforms lacking the Rab3-binding domain induce long lasting currents but block neurotransmitter vesicle anchoring in voltage-dependent P/Q-type Ca^{2+} channels. *J. Biol. Chem.* **285**, 21750–21767
42. Kaeser, P.S., Deng, L., Wang, Y., Dulubova, I., Liu, X., Rizo, J., and Südhof, T.C. (2011) RIM proteins tether Ca^{2+} channels to presynaptic active zones via a direct PDZ-domain interaction. *Cell* **144**, 282–295
43. Han, Y., Kaeser, P.S., Südhof, T.C., and Schneggenburger, R. (2011) RIM determines Ca^{2+} channel density and vesicle docking at the presynaptic active zone. *Neuron* **69**, 304–316
44. Irie, M., Hata, Y., Takeuchi, M., Ichtchenko, K., Toyoda, A., Hirao, K., Takai, Y., Rosahl, T.W., and Südhof, T.C. (1997) Binding of neuroligins to PSD-95. *Science* **277**, 1511–1515
45. Niidome, T., Teramoto, T., Murata, Y., Tanaka, I., Seto, T., Sawada, K., Mori, Y., and Katayama, K. (1994) Stable expression of the neuronal BI (class A) calcium channel in baby hamster kidney cells. *Biochem. Biophys. Res. Commun.* **203**, 1821–1827
46. Wakamori, M., Yamazaki, K., Matsunodaira, H., Teramoto, T., Tanaka, I., Niidome, T., Sawada, K., Nishizawa, Y., Sekiguchi, N., Mori, E., Mori, Y., and Imoto, K. (1998) Single tottering mutations responsible for the neuropathic phenotype of the P-type calcium channel. *J. Biol. Chem.* **273**, 34857–34867
47. Chen, J., Billings, S.E., and Nishimune, H. (2011) Calcium channels link the muscle-derived synapse organizer laminin β2 to Bassoon and CAST/Erc2 to organize presynaptic active zones. *J. Neurosci.* **31**, 512–525
48. Billings, S.E., Clarke, G.L., and Nishimune, H. (2012) ELKS1 and Ca^{2+} channel subunit β4 interact and colocalize at cerebellar synapses. *NeuroReport* **23**, 49–54

49. Burgess, D.L., Jones, J.M., Meisler, M.H., and Noebels, J.L. (1997) Mutation of the Ca^{2+} channel β subunit gene *Cchb4* is associated with ataxia and seizures in the lethargic (*lh*) mouse. *Cell* **88**, 385–392
50. Buraei, Z. and Yang, J. (2010) The β subunit of voltage-gated Ca^{2+} channels. *Physiol. Rev.* **90**, 1461–1506
51. Fouquet, W., Owald, D., Wichmann, C., Mertel, S., Depner, H., Dyba, M., Hallermann, S., Kittel, R.J., Eimer, S., and Sigrist, S.J. (2009) Maturation of active zone assembly by *Drosophila* Bruchpilot. *J. Cell. Biol.* **186**, 129–145
52. Deken, S.L., Vincent, R., Hadwiger, G., Liu, Q., Wang, Z.W., and Nonet, M.L. (2005) Redundant localization mechanisms of RIM and ELKS in *Caenorhabditis elegans*. *J. Neurosci.* **25**, 5975–5983
53. Ludwig, A., Flockerzi, V., and Hofmann, F. (1997) Regional expression and cellular localization of the α_1 and β subunit of high voltage-activated calcium channels in rat brain. *J. Neurosci.* **17**, 1339–1349
54. Scott, V.E.S., De Waard, M., Liu, H., Gurnett, C.A., Venzke, D.P., Lennon, V.A., and Campbell, K.P. (1996) β subunit heterogeneity in N-type Ca^{2+} channels. *J. Biol. Chem.* **271**, 3207–3212
55. McEnery, M.W., Vance, C.L., Begg, C.M., Lee, W.-L., Choi, Y., and Dubel, S.J. (1998) Differential expression and association of calcium channel subunits in development and disease. *J. Bioenerg. Biomembr.* **30**, 409–418
56. Stanley, E.F., Reese, T.S., and Wang, G.Z. (2003) Molecular scaffold reorganization at the transmitter release site with vesicle exocytosis or botulinum toxin C1. *Eur. J. Neurosci.* **18**, 2403–2407
57. Lee, A., Westenbroek, R.E., Haeseleer, F., Palczewski, K., Scheuer, T., and Catterall, W.A. (2002) Differential modulation of $Ca_v2.1$ channels by calmodulin and Ca^{2+}-binding protein 1. *Nat. Neurosci.* **5**, 210–217